

Prospects for Antineutrino Running at MiniBooNE

M.O. Wascko^a, for the MiniBooNE Collaboration

^aDepartment of Physics and Astronomy,
Louisiana State University, Baton Rouge, LA 70803

MiniBooNE began running in antineutrino mode on 19 January, 2006. We describe the sensitivity of MiniBooNE to LSND-like $\bar{\nu}_e$ oscillations and outline a program of antineutrino cross-section measurements necessary for the next generation of neutrino oscillation experiments. We describe three independent methods of constraining wrong-sign (neutrino) backgrounds in an antineutrino beam, and their application to the MiniBooNE antineutrino analyses.

1. Introduction

MiniBooNE [1] is a neutrino oscillation experiment at Fermilab, designed to confirm or rule out the hypothesis that the LSND $\bar{\nu}_e$ excess [2] is due to $\bar{\nu}_\mu \rightarrow \bar{\nu}_e$ oscillations. A general description of the experiment can be found elsewhere [3]. Heretofore, MiniBooNE has been taking data in neutrino mode, searching for $\nu_\mu \rightarrow \nu_e$ oscillations. However, in some scenarios involving CP and CPT violation, oscillations may occur only in antineutrinos. Thus, searching for oscillations in antineutrinos is a crucial test [4].

Furthermore, the search for CP violation in the neutrino sector by future off-axis experiments [5, 6] requires $\bar{\nu}_\mu \rightarrow \bar{\nu}_e$ oscillation measurements, as well as $\nu_\mu \rightarrow \nu_e$. The signature for CP violation is an asymmetry in these oscillation probabilities, but this can only be confirmed if the precision of the ν and $\bar{\nu}$ cross sections are smaller than the observed asymmetry. There are few ν cross section data published [7] to date, but even fewer measurements of low energy $\bar{\nu}$ cross sections. We will need more and better data if we hope to find CP violation in the neutrino sector.

Table 1 lists the expected antineutrino event statistics for 2×10^{20} protons on target (POT) of $\bar{\nu}$ running with MiniBooNE [3,8], based on the nuance Monte Carlo [9]. Rates are listed for both right-sign (RS) and wrong-sign (WS) interactions. Note that wrong-signs comprise $\sim 30\%$ of the total events in antineutrino mode, as illustrated in Figure 1. To constrain the wrong-sign

Table 1

Event rates expected in MiniBooNE $\bar{\nu}$ running with 2×10^{20} POT assuming a 550 cm fiducial volume, before cuts. Listed are the expected right-sign (RS) and wrong-sign (WS) events for each reaction channel.

Reaction	$\bar{\nu}_\mu$ (RS)	ν_μ (WS)
CC QE	32,476	11,234
NC elastic	13,329	4,653
CC resonant $1\pi^-$	7,413	0
CC resonant $1\pi^+$	0	6,998
CC resonant $1\pi^0$	2,329	1,380
NC resonant $1\pi^0$	3,781	1,758
NC resonant $1\pi^+$	1,414	654
NC resonant $1\pi^-$	1,012	520
NC coherent $1\pi^0$	2,718	438
CC coherent $1\pi^-$	4,487	0
CC coherent $1\pi^+$	0	748
other (multi- π , DIS)	2,589	2,156
total	71,547	30,539

backgrounds, MiniBooNE has developed several new analysis techniques. We describe three methods below and detail their application to $\bar{\nu}$ cross section measurements at MiniBooNE.

2. Constraining Wrong Sign Events

For charged current (CC) interactions, neutrino events are typically distinguished from antineutrino events by identifying the charge of the

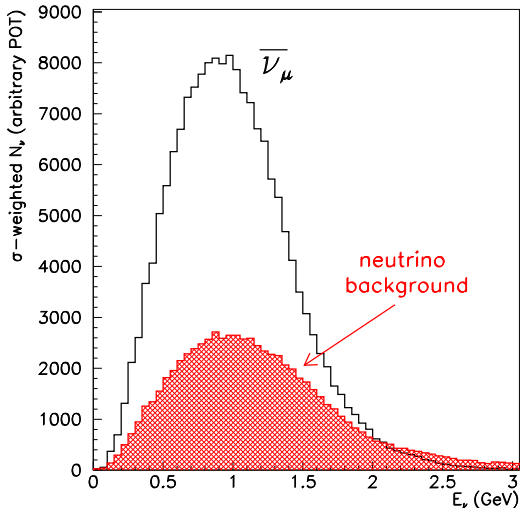


Figure 1. Comparison of cross section weighted right sign (black histogram) and wrong sign (red cross-hatched histogram) fluxes in antineutrino mode.

outgoing muon. MiniBooNE, which has no magnetic field, cannot distinguish ν from $\bar{\nu}$ interactions on an event-by-event basis. Instead, we have developed several novel techniques for measuring WS backgrounds in antineutrino mode data; this will allow more precise $\bar{\nu}$ cross section measurements. The WS content is constrained by three measurements: muon angular distributions in quasi-elastic (CC QE) events; muon lifetimes; and the measured rate of CC single charged pion (CC1 π^+) events [8]. Combined, these three independent measurements (each with different systematic uncertainties) offer a very powerful constraint on the neutrino backgrounds in antineutrino mode (Table 2).

2.1. Muon Angular Distributions

The most powerful wrong-sign constraint comes from the observed direction of outgoing muons in CC QE interactions. Neutrino and antineutrino events exhibit distinct muon angular distributions. Due to the antineutrino helicity, the distribution of final state muons in $\bar{\nu}_\mu$ QE

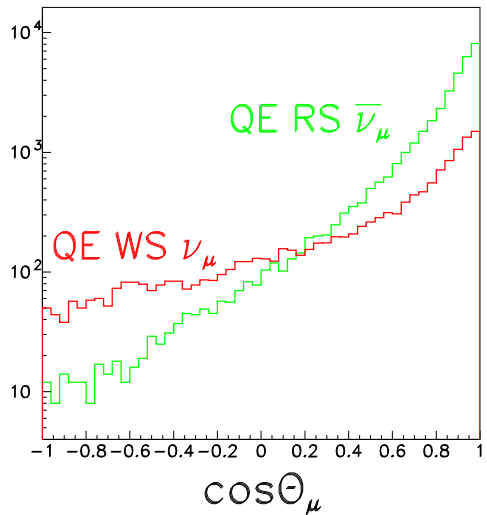


Figure 2. Generated muon angular distributions for CC QE right-sign $\bar{\nu}_\mu$ and wrong-sign ν_μ interactions in antineutrino mode running at MiniBooNE.

events is more forward peaked than that from ν_μ interactions. This is illustrated in Figure 2, which shows the angle of the out-going lepton with respect to the neutrino beam axis for both ν_μ and $\bar{\nu}_\mu$ CC QE events from the nuance Monte Carlo [9].

In order to use this technique to constrain the WS background, the angular resolution for muons must be sufficiently good to separate the two populations. MiniBooNE's angular resolution is measured using the cosmic muon calibration system, which consists of a muon tracker hodoscope placed above the detector. Figure 3 shows the 4° angular resolution of muons between 400 and 500 MeV. This resolution is sufficient to allow exploitation of the angular differences in the CCQE outgoing muons distributions. The angular distributions can be fitted to extract the wrong-sign contribution. Analysis of our Monte Carlo data sets indicates that the wrong-sign content can be measured using this technique, with a statistical uncertainty of 5% of itself [10]. This is illustrated in Figure 4, which shows the reconstructed angle of the out-going lepton with respect to the neu-

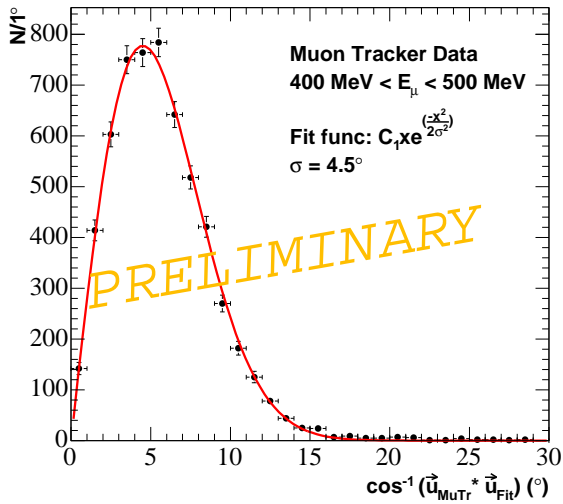


Figure 3. Angular resolution of cosmic muons in MiniBooNE measured using the muon tracker calibration system. The plot shows the angle between the reconstructed muon direction from the tank event fitter and the direction from the muon tracker. This plot shows only events with reconstructed kinetic energy between 400 and 500 MeV, pointed into the fiducial volume of the tank. The fitted width of the distribution is 4.5 degrees, and the intrinsic resolution of the muon tracker is 2 degrees. Assuming the resolutions add in quadrature, this yields an angular resolution of 4 degrees for the tank event fitter.

trino beam axis for both ν_μ and $\bar{\nu}_\mu$ CC QE events generated with the MiniBooNE Monte Carlo, after all selection cuts have been applied. Including systematic uncertainties and (non-QE) backgrounds increases the uncertainty on the WS extraction only to 7%.

2.2. Muon Lifetimes

A second constraint results from measuring the rate at which muons decay in the MiniBooNE detector. Due to an 8% μ^- capture probability in mineral oil, negatively and positively charged muons exhibit different effective lifetimes ($\tau = 2.026 \mu\text{s}$ for μ^- [11] and $\tau = 2.197 \mu\text{s}$ for μ^+ [12]). To extract the WS fraction, one simply fits the

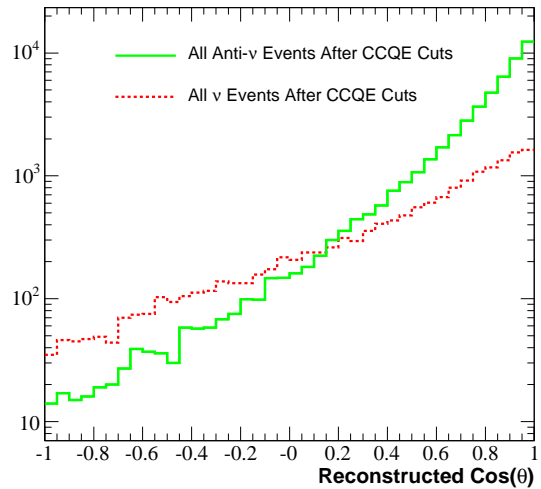


Figure 4. Reconstructed muon angular distributions for CC QE right-sign $\bar{\nu}_\mu$ and wrong-sign ν_μ interactions in antineutrino mode at MiniBooNE.

muon lifetime with a sum of two exponentials, with the extracted fraction of each exponential term giving the fraction of RS or WS events. For CCQE events, we find that the wrong-sign contribution can be extracted with a 30% statistical uncertainty based solely on this lifetime difference and negligible systematic uncertainties. While not as precise as fits to the muon angular distributions, this particular constraint is unique, as it is independent of kinematics.

2.3. CC Single Pion Event Sample

Our third wrong-sign constraint employs the fact that antineutrinos do not create $\text{CC}1\pi^+$ events in the detector—these all stem from neutrinos (Table 1). MiniBooNE identifies $\text{CC}1\pi^+$ events by tagging the two decay electrons that follow the primary neutrino interaction, one from the μ^- and one from the π^+ decay [13]. However, $\text{CC}1\pi^-$ events do not pass this requirement because all the emitted π^- 's which stop in the detector descend into atomic orbits around carbon nuclei and are instantly captured, leaving no decay electrons [14]. The π^- decay in flight rate is much smaller than the rate of π^+ decays at

Table 2

Wrong-sign extraction uncertainties as obtained from various independent sources in the $\bar{\nu}$ data. The resultant systematic uncertainty on $\bar{\nu}$ cross section measurements is obtained by assuming that wrong-signs comprise 30% of the total events.

Measurement	WS uncertainty	resultant error on $\sigma_{\bar{\nu}}$
CC QE $\cos\theta_{\mu}$	7%	2%
CC $1\pi^+$ cuts	15%	5%
muon lifetimes	30%	9%

rest [14]. Thus, applying the two Michel cut to the full sample, which is 70% antineutrino (RS) interactions, yields an 85% pure sample of WS neutrino events.

Assuming conservative uncertainties for the antineutrino background events and the CC $1\pi^+$ cross section, which is currently being measured by MiniBooNE, we expect a 15% uncertainty on the wrong-sign content in the beam given 2×10^{20} POT. This constraint is complementary to the muon angular distributions, because CC $1\pi^+$ events stem mainly from resonance decays, thus constraining the wrong-sign content at larger neutrino energies.

3. CC Quasi-Elastic Scattering

MiniBooNE expects more than 40,000 QE interactions in antineutrino mode with 2×10^{20} POT before cuts. Using the same QE event selection criteria as the previously reported MiniBooNE neutrino analysis [15] yields a sample of $\sim 19,000$ events, with 75% QE purity with both WS and RS events.

Assuming the above wrong-sign constraints and conservative errors on the ν flux, backgrounds, and event detection, we expect a MiniBooNE measurement of the $\bar{\nu}_{\mu}$ QE cross section to better than 20% with 2×10^{20} POT.

4. NC Single Pion Production

$\bar{\nu}_{\mu}$ neutral current (NC) π^0 production is one of the largest backgrounds to future $\bar{\nu}_{\mu} \rightarrow \bar{\nu}_e$ oscilla-

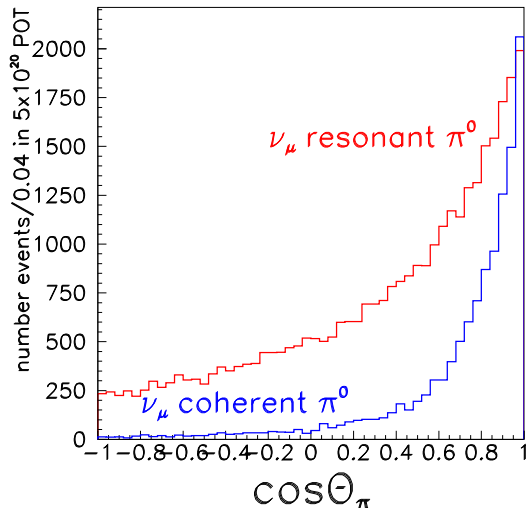


Figure 5. Generated π^0 angular distributions for NC ν scattering [9]. This is the angle of the outgoing π^0 in the lab with respect to the ν direction.

tion searches. There has been only one published measurement of the absolute rate of this channel, with 25% uncertainty at 2 GeV [16].

Applying MiniBooNE's ν_{μ} NC π^0 cuts [17] with no modifications leaves a sample of antineutrino NC π^0 events with a similar event purity and efficiency. After this selection, we expect 1,650 $\bar{\nu}_{\mu}$ resonant NC π^0 events and 1,640 $\bar{\nu}_{\mu}$ coherent NC π^0 events assuming 2×10^{20} POT and the Rein and Sehgal model of coherent pion production [9,18]. Coherent pion production has a characteristic pion angular distribution that allows it to be distinguished from resonant production, as illustrated in Figures 5 and 6. Moreover, the previously mentioned figures illustrate that the distinctiveness of the angular distributions should be even more marked in antineutrino running, which increases the value of antineutrino data for understanding coherent production. The background of ~ 1000 WS events will be determined by the constraints on the wrong-sign content in the beam as described in Section 2 and the measurement of the ν_{μ} NC π^0 cross section from MiniBooNE neutrino data.

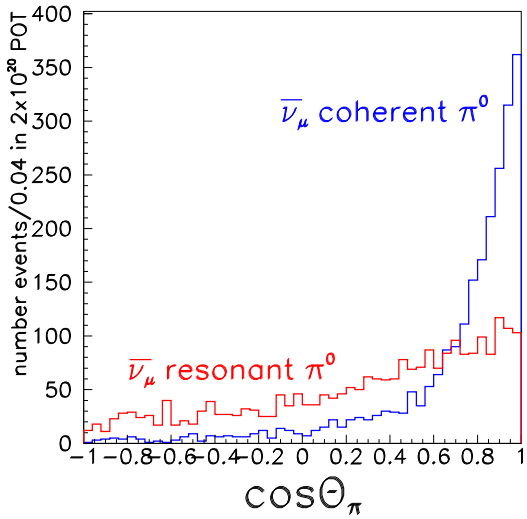


Figure 6. Generated π^0 angular distributions for NC $\bar{\nu}$ scattering [9]. This is the angle of the outgoing π^0 in the lab with respect to the ν direction. The coherently produced π^0 's are more forward peaked than the resonant π^0 's in both cases.

5. CC Single Pion(CC1 π^-) Production

MiniBooNE expects roughly 7,000 resonant CC $1\pi^-$ with 2×10^{20} POT before cuts. As discussed above, almost all of the emitted π^- 's will be absorbed by carbon nuclei, and will therefore not be selected by the CC1 π^+ cuts. Nevertheless, these events still have a signature: two Cherenkov rings (one each from the μ^+ and π^-) and one Michel electron in the vicinity of the μ^- . The selection efficiency and purity of such events is unknown at this time. Further investigation is currently underway.

6. Oscillation Sensitivity

Although MiniBooNE has been searching for oscillations in neutrino mode, the LSND oscillation signal was actually an excess of antineutrino events. Because of the potential for finding CP violation in the neutrino sector, it is imperative that MiniBooNE test the LSND oscillation hy-

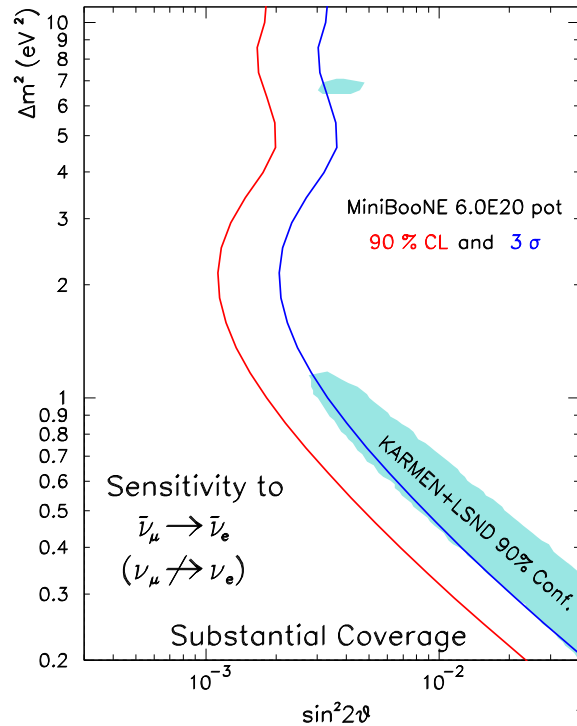


Figure 7. Sensitivity to $\bar{\nu}_\mu \rightarrow \bar{\nu}_e$ oscillations assuming no $\nu_\mu \rightarrow \nu_e$ oscillations using an energy spectrum fit. Shown in blue is the allowed 90% CL region from a joint analysis of the KARMEN and LSND $\bar{\nu}_\mu \rightarrow \bar{\nu}_e$ oscillations results [20].

pothesis with antineutrino data [4].

Figure 7 shows an estimate of the MiniBooNE sensitivity to $\bar{\nu}_\mu \rightarrow \bar{\nu}_e$ oscillations under the assumption that $\nu_\mu \rightarrow \nu_e$ oscillations do not occur, i.e. assuming MiniBooNE sees no ν_e appearance signal. Here, we compare the sensitivity to the joint KARMEN-LSND region ($\bar{\nu}$ only) [20], not the full LSND allowed region ($\nu + \bar{\nu}$). This is a statistics-limited search; further running is needed beyond the 2×10^{20} POT assumed in the preceding sections in order to test the LSND hypothesis. This sensitivity shown assumes 6×10^{20} POT.

7. Conclusions

We have developed three techniques for determining the wrong-sign background in antineutrino mode. The resulting systematic error on any given $\bar{\nu}$ cross section measurement due to the wrong sign contamination should be less than 2% averaged over the entire flux, which is remarkable for a detector which does not possess event-by-event sign selection. Given this redundant approach, the wrong-sign contamination should not be considered prohibitive to producing meaningful antineutrino cross section [8] and oscillation measurements [8,19,21] at MiniBooNE. These techniques may also be useful for other experiments without magnetized detectors which have plans to study antineutrino interactions (*e.g.* T2K, NO ν A, Super-K).

MiniBooNE began running in antineutrino mode on 19 January, 2006, and is currently approved to run for one more year. In order to truly confirm or rule out the LSND oscillation hypothesis, MiniBooNE needs 6×10^{20} POT, which will require additional years of running.

8. Acknowledgments

The author is pleased to acknowledge the collaborative efforts of J.M. Link, H.A. Tanaka, and G.P. Zeller in developing the ideas in this work. The author would also like to express gratitude to the organizers of NuInt05 for their generous travel support.

The MiniBooNE collaboration gratefully acknowledges support from various grants and contracts from the Department of Energy and the National Science Foundation. The author was supported by grant number DE-FG02-91ER0617 from the Department of Energy.

REFERENCES

1. FERMILAB-PROPOSAL-0898, Dec 1997, *nucl-ex/9706011*.
2. A. Aguilar *et al.*, Phys. Rev. **D 64**, 112007 (2001.)
3. A. A. Aguilar-Arevalo *et al.*, “The MiniBooNE Run Plan” (2003), <http://www-boone.fnal.gov/publicpages/runplan.ps.gz>.
4. APS Multi-Divisional Study in Neutrino Physics, <http://www.aps.org/neutrino/>.
5. K. Nishikawa *et al.* (T2K Collaboration), KEK Report (2003), <http://neutrino.kek.jp/jhfnu>.
6. FERMILAB-PROPOSAL-0929, March 2004, *hep-ex/0503053*.
7. G. P. Zeller, NuInt02, *hep-ex/0312061*.
8. MiniBooNE Collaboration, “Addendum to the MiniBooNE Run Plan,” <http://www-boone.fnal.gov/publicpages/loi.ps.gz>.
9. D. Casper, Nucl. Phys. Proc. Suppl. **112**, 161 (2002), *hep-ph/0208030*.
10. H.A. Tanaka, “Estimating WS Content in Negative Polarity Horn Data”, BooNE Memo (2004). For more information on the BooNE Memos and Technical Notes, contact the MiniBooNE spokespeople, J. M. Conrad or W. C. Louis.
11. T. Suzuki *et al.*, Phys. Rev. **C35**, 2122 (1987).
12. S. Eidelman *et al.*, Phys. Lett. **B592**, 33 (2004).
13. M. O. Wascko, “ ν_{μ} -Carbon CC1 π^{+} Cross Section Measurement at MiniBooNE”, these proceedings.
14. C. Athanassopoulos *et al.*, Nucl. Instr. Meth. **A388** (1997) 149-172.
15. J. Monroe, Moriond 2004, *hep-ex/0406048*.
16. H. Faissner, *et al.*, Phys. Lett. **126B**, 230 (1983).
17. J. L. Raaf, NuInt04, *hep-ex/0408015*.
18. D. Rein and L. M. Sehgal, Nucl. Phys. **B223**, 29 (1983).
19. J. Monroe, “ ν_{μ} Disappearance Studies for the Fall 2004 LoI”, BooNE Memo (2004).
20. E. D. Church *et al.*, Phys. Rev. **D66**, 013001 (2002), *hep-ex/0203023*.
21. A. A. Aguilar-Arevalo, “MiniBooNE Osc. Sensitivity in $\bar{\nu}$ Mode”, BooNE Memo (2004).